This is the accepted manuscript made available via CHORUS. The article has been published as:

Continuous Wigner-Mott transitions at math xmlns="http://www.w3.org/1998/Math/MathML">mrow>mi>ν/mi>mo>=/mo>mn>1/mn>mo>//mo>mn>5/mn>/mrow>/math>

Thomas G. Kiely and Debanjan Chowdhury

Phys. Rev. B **110**, L241112 — Published 26 December 2024

DOI: 10.1103/PhysRevB.110.L241112

Continuous Wigner-Mott Transitions at $\nu = 1/5$

Thomas G. Kiely and Debanjan Chowdhury
Department of Physics, Cornell University, Ithaca, New York 14853, USA.

Electrons can organize themselves into charge-ordered states to minimize the effects of long-ranged Coulomb interactions. In the presence of a lattice, commensurability constraints lead to the emergence of incompressible Wigner-Mott insulators at various rational electron fillings, $\nu = p/q$. The mechanism for quantum fluctuation-mediated melting of the Mott insulators with increasing electron kinetic energy remains an outstanding problem. Here, using matrix product state techniques, we analyze the bandwidth-tuned transition out of the Wigner-Mott insulator at $\nu = 1/5$ in an extended Hubbard model on infinite cylinders of varying circumference. For the two-leg ladder, the transition from the Mott insulator to the Luttinger liquid proceeds via a distinct intermediate phase with gapless Cooper-pairs and gapped electronic excitations. The resulting Luther-Emery liquid is the analog of a strongly fluctuating superconductor. We place these results in the context of a low-energy bosonization based theory for the transition. On the five-leg cylinder, we provide numerical evidence for a direct continuous transition between the Wigner-Mott insulator and a metallic phase across which the spin and charge-gaps vanish simultaneously. We comment on the connections to ongoing experiments in dual-gated bilayer moiré transition metal dichalcogenide materials.

Introduction.- The emergence of Wigner-Mott insulators at a partial commensurate filling of electronic bands is one of the hallmarks of an interaction-induced phenomenon [1]. Despite being an old problem, much remains to be understood about how a Wigner-Mott (WM) insulator emerges from a Landau-Fermi liquid (FL) at a fixed electronic filling (ν) as a function of increasing strength of interactions. The FL metal hosts an electronic Fermi surface whose area is fixed by Luttinger's theorem [2, 3]. On the other hand, the WM insulator does *not* host any electronic Fermi surface and spontaneously breaks space-group (and, possibly, spin-rotation) symmetries. Given these differences, one might expect that the most common scenario would be for the metal-insulator transition to be first-order in nature, which is seen in many solid-state materials [4]. An alternative "weak-coupling" perspective suggests that the transition can proceed via intermediate metallic phases with broken translational symmetry and an even number of electrons in the enlarged unit-cell. Examples of both classes of transitions, including the additional effects of disorder, have been analyzed in a large body of earlier work [5–8]. The most intriguing scenario involves a direct continuous transition between a symmetry-preserving FL metal and a WM insulator. As a matter of principle, such continuous transitions can be described using quantum field theoretic methods involving fractionalized degrees of freedom and emergent gauge-fields [9, 10], but they typically rely on artificial limits to make computational progress.

In this letter, we study the transition(s) between a WM insulator and a FL metal at a fixed filling $\nu = 1/5$ for spinful electrons on the triangular lattice using infinite matrix product state (MPS) techniques [11, 12]. In the strong-coupling regime, superexchange leads to a spin-singlet Mott-insulating ground state with finite spin and charge gaps, Δ_s, Δ_c, respectively; see Fig. 1. Starting with the fully-gapped Mott insulator, which can be efficiently represented using MPS, we address the quantum fluctuation-induced melting with increasing single-electron bandwidth. In particular, are there intermediate gapless phases distinct from a symmetry-preserving FL metal (Fig. 1a), or is there a direct transition to the FL across which Δ_s, Δ_c vanish simultaneously (Fig. 1b)?

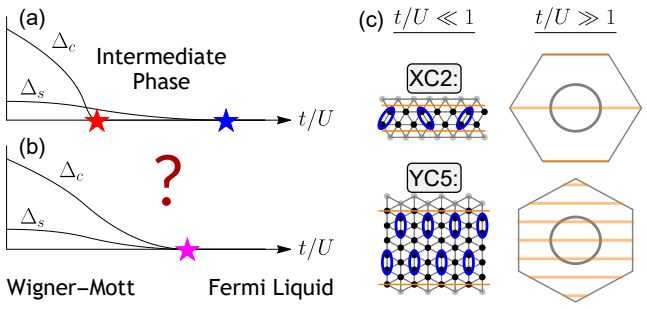


FIG. 1. Schematic for two possible scenarios for continuous bandwidth-tuned Mott transitions at $\nu = 1/5$, where Δ_c, Δ_s vanish at: (a) two separate QCPs, with an intermediate gapless phase, or (b) the same QCP but with distinct critical exponents. (c) The two quasi-2D infinite cylinder geometries, XC2 and YC5, along with the respective Mott insulators ($t/U \ll 1$) and the electronic Fermi surface in the metallic phase ($t/U \gg 1$). The blue ovals denote singlet bonds and the orange lines denote cuts through the electronic Fermi surface, corresponding to the allowed momentum modes around the cylinder circumference.

With increasing quantum fluctuations, the spin-singlets in the Wigner-Mott insulator can melt into delocalized, strongly fluctuating Cooper-pairs before breaking apart to reveal the electronic excitations. For a particular set of microscopic interaction parameters, we find compelling evidence for this two-step transition on two-leg ladders where the intervening Luther-Emery liquid [13, 14] hosts a gap to single-electron excitations, but not to the spin-singlet Cooper pairs. We emphasize that this is a "strong-coupling" route to engineering superconductivity in a model with purely repulsive interactions, without the need for any microscopic attraction. This curious result derives from the Wigner-Mott state, which can be understood as a crystal of localized Cooper-pairs (see Fig. 1c). The recent report of superconductivity in twisted WSe_2 obtained by melting a correlated insulator [15] at $\nu = 1$ is an

interesting experimental example of similar phenomenology; see also Ref. [16]. Notably, the conditions under which these pairing correlations emerge (at low-density and with long-range interactions) are markedly distinct from prior reports of pairing correlations at weak coupling [17, 18] or at unit filling [19–21] in two-leg ladders, and they differ from recent theoretical predictions under comparable conditions [22].

On the five-leg cylinder and for a similar choice of parameters, we find evidence for a *direct continuous transition* between the Wigner-Mott insulator with broken translational symmetry and a gapless metallic phase. Such a transition is seemingly at odds with any Landau-Ginzburg-Wilson-based paradigm for continuous quantum phase transitions, as there is no *a priori* reason for the spin and charge orders to vanish and the electronic Fermi surface to appear simultaneously. This result is corroborated in part by a non-trivial scaling collapse associated with the extracted spin and charge "gaps", respectively.

Experimental motivation.- Bilayers of transition metal dichalcogenides (TMDs) realize an effective moiré triangular lattice, and have been used to study a bandwidth-tuned continuous metal-Mott insulator transition at $\nu = 1/2$ [23, 24]. In parallel, a number of experiments using moiré TMDs have reported evidence for a plethora of Wigner-Mott insulators at electron fillings $\nu = 1/6,\ 1/5,\ 1/4$ etc., induced by the screened long-range Coulomb interactions [25–27]. Wigner crystals in the absence of a moiré potential have been reported across different platforms in earlier work [28–32]. While the nature of the electron spin-configuration, and its possible ordering, is presently unclear for all of these WM insulators, the charge-order for $\nu = 1/6$ has been imaged directly [33]. The competing spin-exchange interactions are highly frustrated and the ordering (or lack thereof) is a delicate question [34–36]. In the context of moiré systems, previous theoretical effort has focused on the crystalline regime deep in the Mott insulator [37, 38]; Hartree-Fock [39–41], classical Monte-Carlo [42], and DMRG-based [43] methods have also been used to study the competition between spin and charge-orderings over a range of coupling strength and density. Momentum-space-based exact diagonalization methods have also been employed to study the metal-insulator transition for a host of other fillings [44, 45]. The Mott insulator [1] at $\nu = 1/5$ provides a useful starting point to study the onset of electron delocalization and melting of the spin-gap, going beyond any Hartree-Fock or classical Monte-Carlo-based approach.

Model & Method.- We study the ground state phase diagram of the extended Hubbard model on the triangular lattice, given by

$$H = H_{\text{kin}} + H_{\text{int}}, \tag{1a}$$

$$H_{\text{kin}} = -t \sum_{\langle \boldsymbol{r},\boldsymbol{r}'\rangle,\sigma} \left(c^\dagger_{\boldsymbol{r}\sigma} c_{\boldsymbol{r}'\sigma} + \text{H.c.} \right) - \mu \sum_{\boldsymbol{r}} n_{\boldsymbol{r}}, \tag{1b}$$

$$H_{\text{int}} = U \sum_{\boldsymbol{r}} n_{\boldsymbol{r}\uparrow} n_{\boldsymbol{r}\downarrow} + \frac{1}{2} \sum_{\boldsymbol{r}\neq\boldsymbol{r}'} V(\boldsymbol{r}-\boldsymbol{r}')\, n_{\boldsymbol{r}} n_{\boldsymbol{r}'}. \tag{1c}$$

Here the electron creation and annihilation operators at site $\boldsymbol{r}$ with spin σ are denoted $c^\dagger_{\boldsymbol{r}\sigma}$, $c_{\boldsymbol{r}\sigma}$, respectively. The on-site interaction, U, and further neighbor interactions, $V(\boldsymbol{r})$, are kept fixed, with the latter determined by the screened Coulomb interaction in bilayer TMD experiments [23–25]. For our calculations, we truncate $V(\boldsymbol{r})$ at fourth-nearest-neighbor interactions on the triangular lattice with $V_2/V_1 \approx 0.512$, $V_3/V_1 \approx 0.423$, and $V_4/V_1 \approx 0.284$, where V_n is the n^{th} nearest-neighbor interaction strength [46]. We choose $V_1/U = 0.5$. The single electron hopping is t, and the chemical potential, μ, couples to the total electron density with $n_{\boldsymbol{r}} = \sum_\sigma c^\dagger_{\boldsymbol{r}\sigma} c_{\boldsymbol{r}\sigma}$. In the remainder of this manuscript, we focus on the electron filling fraction $\nu = 1/5$ and in the zero-magnetization sector. The phase diagram is then studied by varying t at fixed filling and interaction.

We make use of infinite matrix product state (iMPS) techniques on two quasi-2D geometries: the two-leg ladder (XC2) and the five-leg cylinder (YC5). The geometries are shown schematically in Fig. 1(c). We numerically determine variational ground states as function of the iMPS bond dimension, χ [47, 48]. Wherever possible, we extrapolate our results in the limit $\chi \to \infty$. See [46] for further details.

Two-leg ladders.- We perform calculations with the XC2 geometry for two different choices of the hopping parameters. We denote the hopping amplitude along the long direction t and the amplitude along the short direction t' (see Fig. 1). For (i) $t = t'$, the bandstructure leads to 2 Fermi points (FP), as in Fig. 2a, while for (ii) $t' = 6t$ there are 4 FP as in Fig. 2f. Let us denote the metallic phase in the corresponding bosonized model as $C\alpha S\beta$, where α (β) denote the number of charge (spin) modes, respectively. For both cases, we find a Mott insulator on the two-leg ladder for $U/t \gg 1$ and a metallic Luttinger liquid (LL) for $U/t \ll 1$ (see Fig. 1c). We do *not*, however, find a direct transition between these phases – rather, with increasing t/U, the WM insulator first transitions into an intermediate phase with *gapless* spin-singlet Cooper-pair excitations and a gap to spin excitations.Further increasing t, there is a subsequent transition at t_{c2}/U where the spin gap closes and we recover the LL. Thus, the melting of the WM insulator fits into the schematic shown in Fig. 1a. For case (i), the Mott insulator melting transition follows the sequence $C0S0 \to C1S0 \to C1S1$, while for case (ii), the sequence is given by $C0S0 \to C1S0 \to C2S2$. In both cases, the transition proceeds via an intermediate Luther-Emery liquid ($C1S0$). This is the fluctuating "superconducting" phase, that appears in a purely repulsive model without *any* retardation effects by melting the localized spin-singlet Cooper pairs. This two-step transition is summarized in Fig. 2 for cases (i)

[1] The same filling is denoted $\nu_c = 2/5$ in Ref. [25], measured relative to the full filling of the band ($\nu_c = 2$).

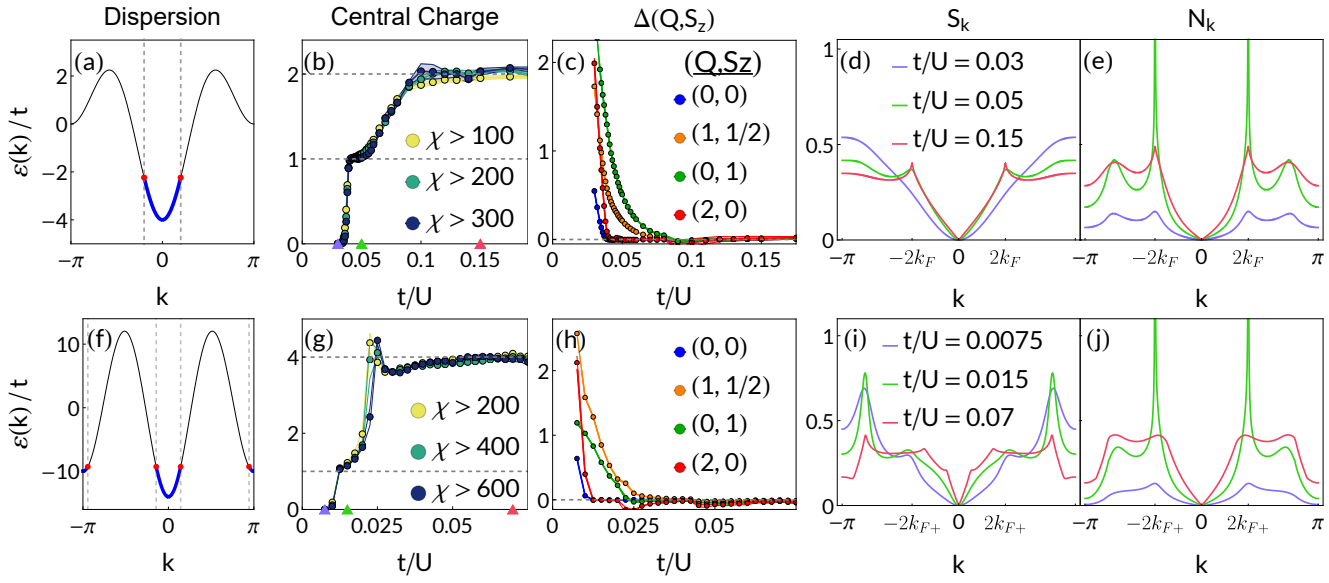


FIG. 2. The two-step Mott-metal transition, as shown in Fig. 1a, on the XC2 geometry. Panels (b)-(e) support the scenario $C0S0 \to C1S0 \to C1S1$ for the dispersion shown in (a) with 2 Fermi points. Similarly, panels (g)-(h) support the scenario $C0S0 \to C1S0 \to C2S2$ for the dispersion shown in (f) with 4 Fermi points. The $C1S0$ phase is a Luther-Emery liquid. Conformal central charge (C) shows a sharp transition from $C = 0$ to $C = 1$ across (b) $t_{c1}/U = 0.04$ (for (a)), and (g) $t_{c1}/U = 0.01$ (for (f)). There is a subsequent gradual increase from (b) $C = 1$ to $C = 2$ across $t_{c2}/U \approx 0.1$ (for (a)), and (g) $C = 1$ to $C = 4$ across $t_{c2}/U \approx 0.024$ (for (f)). Different colors represent C obtained by removing varying number of low-χ states (see main text). (c) and (h) Extrapolated spectral gaps, $\Delta(Q, S_z; \chi)$, in different symmetry sectors across the phase diagram for the dispersions in (a) and (f), respectively. Below t_{c1} all symmetry sectors are gapped; between t_{c1} and t_{c2} the spin sectors remain gapped while the $(Q, S_z) = (0, 0)$ and $(2, 0)$ gaps vanish. For $t > t_{c2}$ all sectors are gapless. (d),(i) Spin and (e),(j) density structure factors for three representative points in the phase diagram (marked by the '▲' in (b) and (g)). In a gapless sector associated with a specific $\{Q,\ S_z\}$, the corresponding SF$\sim |k|$ for small k and develops singular cusps at $2k_F$, or $2k_{F+} = 2(k_{F1} + k_{F2})$ (see main text).

(panels a-e) and (ii) (panels f-j). As the phenomenology is largely the same, we will limit our discussion in the main text to case (i); please see [46] for a discussion of case (ii) as well as further details on these observables.

We use three diagnostics to study the metal-insulator transition: the conformal central charge, the inverse correlation length, and the static structure factors. The central charge, C, is shown as a function of t/U in Fig. 2b. In the Mott phase, the ground state is gapped and $C = 0$. Across $t_{c1}/U \approx 0.04$ we see a sharp increase in C followed by a plateau around $C \approx 1$. This plateau becomes more prominent at larger bond dimensions (different colors in Fig. 2b). The central charge $C = 1$ is consistent with two gapless modes, while the two-component LL has four gapless modes. Hence, this plateau is strongly suggestive of a distinct intermediate phase. Across $t_{c2}/U \approx 0.1$, the system enters the LL phase with $C = 2$. In [46] we provide an estimate of t_{c1} and t_{c2}, with standard error bars, using a scaling collapse.

The inverse correlation lengths are shown in Fig. 2c. The iMPS variational wavefunction is characterized by a spectrum of correlation lengths, $\{\xi(\chi)\}$, which has been shown to map onto the low-energy excitation spectrum (up to an overall scale factor) as $\chi \to \infty$ [49, 50]. In Fig. 2c, we show the dominant inverse correlation lengths ("gaps") in some of the relevant symmetry sectors, labeled by U(1) charge (Q) and spin (S_z) quantum numbers [51]: $\Delta(Q, S_z) \equiv \lim_{\chi\to\infty} 1/\xi(Q, S_z; \chi)$ [46]. In the Mott phase, all symmetry sectors are gapped. As we cross t_{c1}, the gaps for spinless excitations ($(0, 0)$ and $(2, 0)$) vanish while those for spinful excitations ($(1, 1/2)$ and $(0, 1)$) are finite. This is consistent with $C = 1$ and reveals that the intermediate phase has gapless charge excitations with a gap to spin excitations. Across t_{c2}, all symmetry sectors show a vanishing gap, consistent with the expected behavior in the LL phase.

The density and spin structure factors (SF) are shown in Figs. 2d and e. The spin SF is defined as $\mathcal{S}_k = \frac{1}{5}\sum_{j=1}^{5}\sum_l e^{ilk}\langle \boldsymbol{S}_j \cdot \boldsymbol{S}_{l+j}\rangle$ where j iterates over the 5-site unit cell and $\boldsymbol{S}_j = (1/2)\sum_{\alpha,\beta} c^\dagger_{j,\alpha}\boldsymbol{\sigma}_{\alpha,\beta}c_{j,\beta}$. We define the density SF as $\mathcal{N}_k = \frac{1}{5}\sum_{j=1}^{5}\sum_l e^{ilk}\langle (n_j - \langle n_j\rangle)(n_{l+j} - \langle n_{l+j}\rangle)\rangle$, subtracting off the average density on each site [46]. In the Mott insulator, both the density and spin SF are featureless (non-singular at any k). At small k, they vanish smoothly as $\mathcal{N}_k,\ \mathcal{S}_k \sim k^2$, indicating a finite spin and charge gap, respectively [52]. In the intermediate phase, the spin SF remains featureless while $\mathcal{N}_k \sim |k|$ for small k, indicating that the charge gap has closed. The density SF also develops singular peaks at $\pm 2k_F$ that appear to diverge in the limit $\chi \to \infty$. In the LL phase, both the density and spin SF scale as $\mathcal{N}_k,\ \mathcal{S}_k \sim |k|$ for small k and develop singular cusps at $\pm 2k_F$ [46].

Five-leg cylinder.- To study the effect of an increasing cylinder width, we perform calculations on the YC5 geometry with

isotropic hopping amplitudes. Our results are summarized in Fig. 3. We show both the symmetry-resolved spectrum of inverse correlation lengths (panel (a)), derived from eigenvalues of the MPS transfer matrix, as well as the conformal central charge (panel (b)) across the transition. Data is shown for bond dimensions $\chi = 2400, 2800, 3200$ for all data points; in the vicinity of the transition, we show additional data at $\chi = 3600, 4000$. We omit data below $\chi = 2400$ because it shows strong finite-χ effects [46].

We find evidence of a Wigner-Mott insulating phase for $t/U \lesssim 0.08$ which is well-characterized by the cartoon in Fig. 1c: spatially-separated pairs of electrons that form spin-singlets. This state is characterized by a spin and charge gap, as evidenced by a sharp increase in the inverse correlation lengths across all sectors. For $t/U \gtrsim 0.084$, we find that the inverse correlation lengths in all symmetry sectors appear to vanish uniformly with increasing χ and the central charge (Fig. 3c) approaches $C = 6$, as expected in the gapless FL phase. We emphasize that these inverse correlation lengths are not extrapolated with respect to bond dimension, and hence do not vanish in the FL phase (c.f. Fig. 2). The central charge of 6 is the maximum number of gapless modes for free fermions on the YC5 cylinder, and hence provides strong evidence that we are in the FL phase.

For all χ, the Wigner-Mott insulator melts as t/U is increased; the location at which it melts, however, exhibits some χ dependence. Moreover, we are unable to apply the extrapolation method used in the XC2 geometry [46]; this is likely due to a combination of degeneracies on the cylinder geometry as well as finite-χ effects. Intriguingly, however, we find that the gaps (inverse correlation lengths) exhibit a scaling collapse when *both* $\Delta(Q, S_z)$ and the value of t/U are rescaled by powers of the bond dimension. This hallmark signature of a quantum critical point allows us to approximate both t_c/U as well as the critical exponents. Specifically, we assume that the gaps take the scaling form $\Delta(t_c - t, \chi) \propto \chi^{\zeta/\delta} f((t_c - t)/\chi^{1/\delta})$ near the transition, which implies that $\Delta(t_c - t) \propto (t_c - t)^{\zeta}$ as $\chi \to \infty$. In a field-theoretic setting, the exponent $\zeta = \nu z$, can be naturally expressed in terms of the correlation length (ν) and dynamical exponents (z), respectively, assuming that the transition is truly continuous. We then fit the parameters $\{t_c, \zeta, \delta\}$ within each independent symmetry sector, obtaining an approximate location for the transition as well as the critical exponents. The scaling collapses are shown in Fig. 3c. We fit each symmetry sector independently, finding very close agreement with $t_c/U = 0.081(1)$. Best-fit parameters for the individual sectors are displayed on Fig. 3c and are reported in [46]. Fits are performed by defining a cost function in terms of the residuals from an interpolated scaling function, and error bars come from integrating the associated probability distribution [46, 53]. Smaller error bars on $\{t_c, \zeta, \delta\}$ could be obtained by taking more data on a finer grid, but a more precise location for the transition would likely require going beyond $\chi = 4000$.

Discussion.- In this letter, we have analyzed the quantum melting of a crystalline Wigner-Mott insulator with well formed spin-singlets into a symmetry-preserving metal using

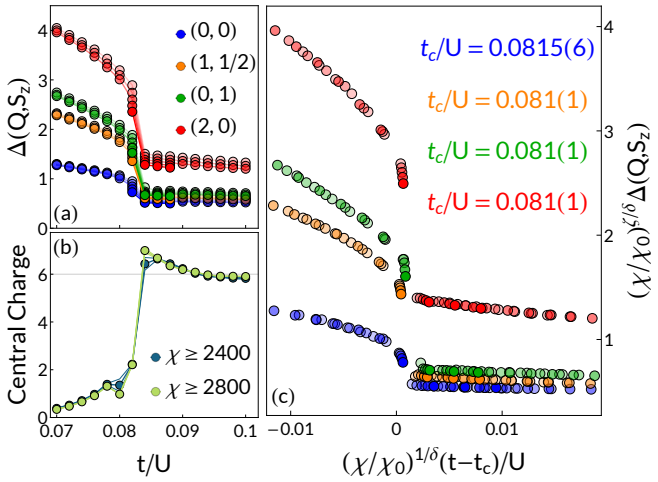


FIG. 3. Mott insulator-metal transition at $\nu = 1/5$ on the YC5 geometry. Panel (a) shows dominant inverse correlation lengths in different symmetry sectors, $\Delta(Q, S_z)$, as a function of t/U. Colors denote different sectors while the opacity denotes the bond dimension; data here is for $\chi = 2400, 2800, 3200, 3600, 4000$. We see that all symmetry sectors exhibit similar behavior, showing a gap for $t/U \lesssim 0.08$ and vanishing smoothly for $t/U \gtrsim 0.084$. Panel (b) shows the central charge, extracted from a linear fit to the entanglement entropy versus correlation length, in the same region. The gapless region has a central charge $C = 6$ on the YC5 geometry, consistent with panel (a), while C vanishes in the gapped region. Panel (c) shows a collapse of the data in panel (a) after rescaling both axes by powers of the bond dimension (for scale, we take $\chi_0 = 3200$). This non-trivial result suggests that the transition is continuous, and allows us to extract critical values of t_c/U within each symmetry sector (shown on plot, see main text for discussion).

iMPS-based methods. Experiments in moiré TMDs are already well-placed to study such transitions in detail in the future. For two-leg ladders, we find clear evidence for an intermediate gapless Luther-Emery phase, which is distinct from the usual Luttinger liquid. This one-dimensional analog of a fluctuating superconductor may enjoy enhanced stability due to the low dimensionality of the system – a true 2D analog would be an interesting subject of future work. In the system studied here, kinetic energy-driven quantum fluctuations favor melting the spin-singlets into a fluctuating (spin-gapped) superconductor without a gap to Cooper-pair excitations. Extending this picture to the case of the recent experiments [15, 16], which observe superconductivity in the vicinity of a correlated insulator, remains an interesting future direction.

We have studied the effect of increasing the spatial extent along the second dimension by analyzing the same problem on five-leg cylinders. There, we find that the intermediate gapless phase vanishes altogether, yielding to a continuous bandwidth-tuned metal-insulator transition. Developing complementary analytical methods in two spatial dimensions, going beyond the usual large-N parton-based approaches, to study these transitions is clearly also desirable in light of our findings. It is especially challenging to describe such continu-

ous metal-insulator transitions in the absence of *any* remnant Fermi surface in the insulating state [54, 55], associated with even neutral (e.g. spinon) excitations [56], as observed in our five-leg cylinders. Investigating the effect of inhomogeneities on transport near this metal-insulator transition, building on previous studies at other fillings [57–59] will be of direct experimental interest. Since there is a tendency towards superconductivity near the melting transition associated with the Wigner-Mott insulator, it is natural to address the fate of the ground state with additional doped holes [60, 61]. Given the proximity to charge-ordered states, the resulting superconductor might also be a pair-density wave [62]. The importance of proximity to the quantum critical point(s), if any, on the associated phenomenology for the doped case also remains an important open question.

Acknowledgements.- DC thanks S. Kim, K.F. Mak, S. Musser, S. Sachdev, T. Senthil, J. Shan and L. Zou for numerous inspiring discussions and collaborations related to continuous metal-insulator transitions. TK thanks E. Mueller for help with the development and implementation of the numerical methods used in this manuscript. We thank S. Musser for clarifying discussions related to the Mott transition on the XC2 geometry, and for useful comments on an earlier version of this manuscript. TK is supported by an NSF grant (PHY-2110250). This work is supported in part by a CAREER grant from the NSF to DC (DMR-2237522).

[1] Neville Mott, *Metal-Insulator Transitions* (CRC Press, London, 1990).

[2] J. M. Luttinger and J. C. Ward, "Ground-state energy of a many-fermion system. ii," Phys. Rev. **118**, 1417–1427 (1960).

[3] Masaki Oshikawa, "Topological approach to luttinger's theorem and the fermi surface of a kondo lattice," Phys. Rev. Lett. **84**, 3370–3373 (2000).

[4] Masatoshi Imada, Atsushi Fujimori, and Yoshinori Tokura, "Metal-insulator transitions," Rev. Mod. Phys. **70**, 1039–1263 (1998).

[5] Reza Jamei, Steven Kivelson, and Boris Spivak, "Universal Aspects of Coulomb-Frustrated Phase Separation," Physical Review Letters **94**, 056805 (2005).

[6] A. Camjayi, K. Haule, V. Dobrosavljevic, and G. Kotliar, "Coulomb correlations and the Wigner–Mott transition," Nature Physics **4**, 932–935 (2008).

[7] A. Amaricci, A. Camjayi, K. Haule, G. Kotliar, D. Tanaskovic, and V. Dobrosavljevic, "Extended Hubbard model: Charge ordering and Wigner-Mott transition," Physical Review B **82**, 155102 (2010).

[8] DinhDuy Vu and S. Das Sarma, "One-dimensional few-electron effective wigner crystal in quantum and classical regimes," Phys. Rev. B **101**, 125113 (2020).

[9] Seth Musser, T. Senthil, and Debanjan Chowdhury, "Theory of a continuous bandwidth-tuned wigner-mott transition," Phys. Rev. B **106**, 155145 (2022).

[10] Yichen Xu, Xiao-Chuan Wu, Mengxing Ye, Zhu-Xi Luo, Chao-Ming Jian, and Cenke Xu, "Interaction-driven metal-insulator transition with charge fractionalization," Phys. Rev. X **12**, 021067 (2022).

[11] J. Ignacio Cirac, David Pérez-García, Norbert Schuch, and Frank Verstraete, "Matrix product states and projected entangled pair states: Concepts, symmetries, theorems," Rev. Mod. Phys. **93**, 045003 (2021).

[12] Ulrich Schollwöck, "The density-matrix renormalization group in the age of matrix product states," Annals of Physics **326**, 96–192 (2011), january 2011 Special Issue.

[13] A. Luther and V. J. Emery, "Backward scattering in the one-dimensional electron gas," Phys. Rev. Lett. **33**, 589–592 (1974).

[14] E. W. Carlson, V. J. Emery, S. A. Kivelson, and D. Orgad, "Concepts in High Temperature Superconductivity," arXiv e-prints , cond-mat/0206217 (2002), arXiv:cond-mat/0206217 [cond-mat.supr-con].

[15] Yiyu Xia, Zhongdong Han, Kenji Watanabe, Takashi Taniguchi, Jie Shan, and Kin Fai Mak, "Unconventional superconductivity in twisted bilayer WSe2," arXiv e-prints , arXiv:2405.14784 (2024), arXiv:2405.14784 [cond-mat.mes-hall].

[16] Yinjie Guo, Jordan Pack, Joshua Swann, Luke Holtzman, Matthew Cothrine, Kenji Watanabe, Takashi Taniguchi, David Mandrus, Katayun Barmak, James Hone, Andrew J. Millis, Abhay N. Pasupathy, and Cory R. Dean, "Superconductivity in twisted bilayer WSe_2," arXiv e-prints , arXiv:2406.03418 (2024), arXiv:2406.03418 [cond-mat.mes-hall].

[17] M. Fabrizio, "Role of transverse hopping in a two-coupled-chains model," Phys. Rev. B **48**, 15838–15860 (1993).

[18] Leon Balents and Matthew P. A. Fisher, "Weak-coupling phase diagram of the two-chain hubbard model," Phys. Rev. B **53**, 12133–12141 (1996).

[19] Elbio Dagotto and T. M. Rice, "Surprises on the way from one- to two-dimensional quantum magnets: The ladder materials," Science **271**, 618–623 (1996).

[20] Kazuhiko Kuroki, Ryotaro Arita, and Hideo Aoki, "Numerical study of a superconductor-insulator transition in a half-filled hubbard chain with distant transfers," Journal of the Physical Society of Japan **66**, 3371–3374 (1997).

[21] Zongsheng Zhou, Weinan Ye, Hong-Gang Luo, Jize Zhao, and Jun Chang, "Robust superconducting correlation against intersite interactions in the extended two-leg hubbard ladder," Phys. Rev. B **108**, 195136 (2023).

[22] Seth Musser and T. Senthil, "Metal to wigner-mott insulator transition in two-leg ladders," Phys. Rev. B **106**, 235148 (2022).

[23] Tingxin Li, Shengwei Jiang, Lizhong Li, Yang Zhang, Kaifei Kang, Jiacheng Zhu, Kenji Watanabe, Takashi Taniguchi, Debanjan Chowdhury, Liang Fu, *et al.*, "Continuous mott transition in semiconductor moiré superlattices," Nature **597**, 350–354 (2021).

[24] Augusto Ghiotto, En-Min Shih, Giancarlo SSG Pereira, Daniel A Rhodes, Bumho Kim, Jiawei Zang, Andrew J Millis, Kenji Watanabe, Takashi Taniguchi, James C Hone, *et al.*, "Quantum criticality in twisted transition metal dichalcogenides," Nature **597**, 345–349 (2021).

[25] Yang Xu, Song Liu, Daniel A Rhodes, Kenji Watanabe, Takashi Taniguchi, James Hone, Veit Elser, Kin Fai Mak, and Jie Shan, "Correlated insulating states at fractional fillings of moiré superlattices," Nature **587**, 214–218 (2020).

[26] Emma C. Regan, Danqing Wang, Chenhao Jin, M. Iqbal Bakti Utama, Beini Gao, Xin Wei, Sihan Zhao, Wenyu Zhao, Zuocheng Zhang, Kentaro Yumigeta, Mark Blei, Johan D. Carlström, Kenji Watanabe, Takashi Taniguchi, Sefaattin Tongay, Michael Crommie, Alex Zettl, and Feng Wang, "Mott and generalized Wigner crystal states in WSe2/WS2 moiré superlattices," Nature **579**, 359–363 (2020).

[27] Xiong Huang, Tianmeng Wang, Shengnan Miao, Chong Wang, Zhipeng Li, Zhen Lian, Takashi Taniguchi, Kenji Watan-

abe, Satoshi Okamoto, Di Xiao, Su-Fei Shi, and Yong-Tao Cui, "Correlated insulating states at fractional fillings of the WS2/WSe2 moiré lattice," Nature Physics **17**, 715–719 (2021).

[28] H. W. Jiang, R. L. Willett, H. L. Stormer, D. C. Tsui, L. N. Pfeiffer, and K. W. West, "Quantum liquid versus electron solid around ν=1/5 landau-level filling," Phys. Rev. Lett. **65**, 633–636 (1990).

[29] Jongsoo Yoon, C. C. Li, D. Shahar, D. C. Tsui, and M. Shayegan, "Wigner crystallization and metal-insulator transition of two-dimensional holes in gaas at $B = 0$," Phys. Rev. Lett. **82**, 1744–1747 (1999).

[30] Md S Hossain, MK Ma, KA Rosales, YJ Chung, LN Pfeiffer, KW West, KW Baldwin, and Mansour Shayegan, "Observation of spontaneous ferromagnetism in a two-dimensional electron system," Proceedings of the National Academy of Sciences **117**, 32244–32250 (2020).

[31] Tomasz Smoleński, Pavel E. Dolgirev, Clemens Kuhlenkamp, Alexander Popert, Yuya Shimazaki, Patrick Back, Xiaobo Lu, Martin Kroner, Kenji Watanabe, Takashi Taniguchi, Ilya Esterlis, Eugene Demler, and Ataç Imamoğlu, "Signatures of wigner crystal of electrons in a monolayer semiconductor," Nature **595**, 53–57 (2021).

[32] You Zhou, Jiho Sung, Elise Brutschea, Ilya Esterlis, Yao Wang, Giovanni Scuri, Ryan J. Gelly, Hoseok Heo, Takashi Taniguchi, Kenji Watanabe, Gergely Zaránd, Mikhail D. Lukin, Philip Kim, Eugene Demler, and Hongkun Park, "Bilayer wigner crystals in a transition metal dichalcogenide heterostructure," Nature **595**, 48–52 (2021).

[33] Hongyuan Li, Shaowei Li, Emma C. Regan, Danqing Wang, Wenyu Zhao, Salman Kahn, Kentaro Yumigeta, Mark Blei, Takashi Taniguchi, Kenji Watanabe, Sefaattin Tongay, Alex Zettl, Michael F. Crommie, and Feng Wang, "Imaging two-dimensional generalized Wigner crystals," Nature **597**, 650–654 (2021).

[34] M. Roger, "Multiple exchange in ^{3}He and in the wigner solid," Phys. Rev. B **30**, 6432–6457 (1984).

[35] Sudip Chakravarty, Steven Kivelson, Cheta Nayak, and Klaus Voelker, "Wigner glass, spin liquids and the metal-insulator transition," Philosophical Magazine B **79**, 859–868 (1999), https://doi.org/10.1080/13642819908214845.

[36] Boris Spivak and Steven A. Kivelson, "Transport in two dimensional electronic micro-emulsions," Annals of Physics **321**, 2071–2115 (2006).

[37] Bikash Padhi, R. Chitra, and Philip W. Phillips, "Generalized wigner crystallization in moiré materials," Phys. Rev. B **103**, 125146 (2021).

[38] Yang Zhang, Tongtong Liu, and Liang Fu, "Electronic structures, charge transfer, and charge order in twisted transition metal dichalcogenide bilayers," Phys. Rev. B **103**, 155142 (2021).

[39] Haining Pan, Fengcheng Wu, and Sankar Das Sarma, "Quantum phase diagram of a moiré-hubbard model," Phys. Rev. B **102**, 201104 (2020).

[40] Haining Pan and Sankar Das Sarma, "Interaction-Driven Filling-Induced Metal-Insulator Transitions in 2D Moiré Lattices," Physical Review Letters **127**, 096802 (2021).

[41] Haining Pan and Sankar Das Sarma, "Interaction range and temperature dependence of symmetry breaking in strongly correlated two-dimensional moiré transition metal dichalcogenide bilayers," Phys. Rev. B **105**, 041109 (2022).

[42] Michael Matty and Eun-Ah Kim, "Melting of generalized Wigner crystals in transition metal dichalcogenide heterobilayer Moiré systems," Nature Communications **13**, 7098 (2022).

[43] Yiqing Zhou, D. N. Sheng, and Eun-Ah Kim, "Quantum phases of transition metal dichalcogenide moiré systems," Phys. Rev. Lett. **128**, 157602 (2022).

[44] Nicolás Morales-Durán, Allan H. MacDonald, and Pawel Potasz, "Metal-insulator transition in transition metal dichalcogenide heterobilayer moiré superlattices," Physical Review B **103**, L241110 (2021).

[45] Nicolás Morales-Durán, Pawel Potasz, and Allan H. MacDonald, "Magnetism and Quantum Melting in Moiré-Material Wigner Crystals," arXiv e-prints , arXiv:2210.15168 (2022), arXiv:2210.15168 [cond-mat.str-el].

[46] "See supplementary material for additional details related to the effect of long-ranged interactions on the charge-ordering in the WM insulator, a brief description of vumps algorithm and our imps computations, the extrapolation of the spectral gaps, central charge, luttinger parameters, computation of the structure factors and error analysis of the critical scaling analysis; includes references [63–76].".

[47] V. Zauner-Stauber, L. Vanderstraeten, M. T. Fishman, F. Verstraete, and J. Haegeman, "Variational optimization algorithms for uniform matrix product states," Phys. Rev. B **97**, 045145 (2018).

[48] Laurens Vanderstraeten, Jutho Haegeman, and Frank Verstraete, "Tangent-space methods for uniform matrix product states," SciPost Phys. Lect. Notes , 7 (2019).

[49] V Zauner, D Draxler, L Vanderstraeten, M Degroote, J Haegeman, M M Rams, V Stojevic, N Schuch, and F Verstraete, "Transfer matrices and excitations with matrix product states," New Journal of Physics **17**, 053002 (2015).

[50] Alexander A. Eberharter, Laurens Vanderstraeten, Frank Verstraete, and Andreas M. Läuchli, "Extracting the speed of light from matrix product states," Phys. Rev. Lett. **131**, 226502 (2023).

[51] Aaron Szasz, Johannes Motruk, Michael P. Zaletel, and Joel E. Moore, "Chiral spin liquid phase of the triangular lattice hubbard model: A density matrix renormalization group study," Phys. Rev. X **10**, 021042 (2020).

[52] Ryan V. Mishmash, Iván González, Roger G. Melko, Olexei I. Motrunich, and Matthew P. A. Fisher, "Continuous mott transition between a metal and a quantum spin liquid," Phys. Rev. B **91**, 235140 (2015).

[53] J. J. Mortensen, K. Kaasbjerg, S. L. Frederiksen, J. K. Nørskov, J. P. Sethna, and K. W. Jacobsen, "Bayesian error estimation in density-functional theory," Phys. Rev. Lett. **95**, 216401 (2005).

[54] Liujun Zou and Debanjan Chowdhury, "Deconfined metallic quantum criticality: A $u(2)$ gauge-theoretic approach," Phys. Rev. Res. **2**, 023344 (2020).

[55] Ya-Hui Zhang and Subir Sachdev, "Deconfined criticality and ghost fermi surfaces at the onset of antiferromagnetism in a metal," Phys. Rev. B **102**, 155124 (2020).

[56] T. Senthil, "Theory of a continuous mott transition in two dimensions," Phys. Rev. B **78**, 045109 (2008).

[57] Yuting Tan, Pak Ki Henry Tsang, and Vladimir Dobrosavljević, "Disorder-dominated quantum criticality in moiré bilayers," Nature Communications **13**, 7469 (2022).

[58] Seongjin Ahn and Sankar Das Sarma, "Disorder-induced two-dimensional metal-insulator transition in moiré transition metal dichalcogenide multilayers," Phys. Rev. B **105**, 115114 (2022).

[59] Sunghoon Kim, T. Senthil, and Debanjan Chowdhury, "Continuous mott transition in moiré semiconductors: Role of long-wavelength inhomogeneities," Phys. Rev. Lett. **130**, 066301 (2023).

[60] P W Anderson, P A Lee, M Randeria, T M Rice, N Trivedi, and F C Zhang, "The physics behind high-temperature super-

conducting cuprates: the 'plain vanilla' version of rvb," Journal of Physics: Condensed Matter **16**, R755 (2004).

[61] Patrick A. Lee, Naoto Nagaosa, and Xiao-Gang Wen, "Doping a mott insulator: Physics of high-temperature superconductivity," Rev. Mod. Phys. **78**, 17–85 (2006).

[62] Daniel F. Agterberg, J.C. Séamus Davis, Stephen D. Edkins, Eduardo Fradkin, Dale J. Van Harlingen, Steven A. Kivelson, Patrick A. Lee, Leo Radzihovsky, John M. Tranquada, and Yuxuan Wang, "The physics of pair-density waves: Cuprate superconductors and beyond," Annual Review of Condensed Matter Physics **11**, 231–270 (2020).

[63] R.M. Noack, S.R. White, and D.J. Scalapino, "The ground state of the two-leg hubbard ladder a density-matrix renormalization group study," Physica C: Superconductivity **270**, 281–296 (1996).

[64] Thomas G. Kiely and Erich J. Mueller, "Superfluidity in the one-dimensional bose-hubbard model," Phys. Rev. B **105**, 134502 (2022).

[65] Steven R. White, "Density matrix renormalization group algorithms with a single center site," Phys. Rev. B **72**, 180403 (2005).

[66] I. P. McCulloch, "Infinite size density matrix renormalization group, revisited," (2008), arXiv:0804.2509 [cond-mat.str-el].

[67] Marek M. Rams, Piotr Czarnik, and Lukasz Cincio, "Precise extrapolation of the correlation function asymptotics in uniform tensor network states with application to the bose-hubbard and xxz models," Phys. Rev. X **8**, 041033 (2018).

[68] Bram Vanhecke, Jutho Haegeman, Karel Van Acoleyen, Laurens Vanderstraeten, and Frank Verstraete, "Scaling hypothesis for matrix product states," Phys. Rev. Lett. **123**, 250604 (2019).

[69] T. G. Kiely and E. J. Mueller, "*manuscript in preparation*," (2023).

[70] Jesse Osborne, Ian P. McCulloch, Bing Yang, Philipp Hauke, and Jad C. Halimeh, "Large-scale 2+1d U(1) gauge theory with dynamical matter in a cold-atom quantum simulator," (2022), arXiv:2211.01380 [cond-mat.quant-gas].

[71] Pasquale Calabrese and John Cardy, "Entanglement entropy and quantum field theory," Journal of Statistical Mechanics: Theory and Experiment **2004**, P06002 (2004).

[72] Thierry Giamarchi, *Quantum Physics in One Dimension* (Oxford University Press, Oxford, 2003).

[73] Manuela Capello, Federico Becca, Michele Fabrizio, and Sandro Sorella, "Mott transition in bosonic systems: Insights from the variational approach," Phys. Rev. B **77**, 144517 (2008).

[74] Hong-Chen Jiang, Zhenghan Wang, and Leon Balents, "Identifying topological order by entanglement entropy," Nature Physics **8**, 902–905 (2012).

[75] Hong-Chen Jiang and Leon Balents, "Collapsing schrödinger cats in the density matrix renormalization group," (2013), arXiv:1309.7438.

[76] Thomas G. Kiely and Erich J. Mueller, "Role of conservation laws in the density matrix renormalization group," Phys. Rev. B **106**, 235126 (2022).